The Boron Buckyball and Its Precursors: An Electronic Structure Study

Arta Sadrzadeh, Olga V. Pupysheva, Abhishek K. Singh, and Boris I. Yakobson*

Department of Mechanical Engineering & Materials Science, Department of Chemistry, Rice University, Houston, Texas 77251

Using ab initio calculations, we analyze electronic structure and vibrational modes of the boron fullerene B_{80}, a stable, spherical cage similar in shape to the well-known C_{60}. There exist several isomers, lying close in structure and energy, with total energy difference within ∼30 meV. We present detailed analysis of their electronic structure and geometry. Calculated radial breathing mode frequency turns out to be 474 cm^{-1}, which can be a characteristic of B_{80} in Raman spectroscopy. Since the B_{80} structure is made of interwoven double-ring clusters, we also investigate double-rings with various diameters. We present their structure and HOMO−LUMO dependence on the diameter, and find out that the gap alternates for different sizes and closes its value for infinite double-ring.

I. Introduction

B_{80} fullerene, also known as the boron buckyball, is energetically one of the most favorable boron clusters studied so far.[1] While essentially icosahedral looking in shape, it has different isomers, all close in energy and geometry, with symmetries such as I_h, T_h, and C_1.[2,3] It is structurally similar to C_{60}, the original buckyball; however, in the B_{80} case there are additional atoms at the centers of the hexagons. Figure 1 shows the total electron density image of this molecule. If confirmed experimentally, with applications such as targeted drug-delivery systems, it might have some impact in applied sciences. We should also mention that boron clusters in general have had application in cancer therapy for years.[4]

B_{80} (again, like C_{60}) can be imagined as a sheet wrapped on a sphere.[5] The most stable structure for the sheet, the α-sheet, was recently reported[6,7] (Figure 2). B_{80} can be viewed as a wrapped α-sheet on a sphere: "empty" hexagons are replaced by 12 pentagonal disclinations required topologically, and strips enclosing them are replaced by B_{30} double rings (DRs). Figure 2a shows how the sheet can be folded to form a pentagonal disclination. Figure 2b highlights the unfolded B_{80} molecule on an α-sheet. If the α-sheet is indeed the most stable structure for the sheet, it should be more stable than any hollow ball and nanotube[7–9] (because of curvature strain energy), and among quasiplanar structures (because of surface energy). B_{80} as the smallest possible spherically wrapped α-sheet cage has a special place in the first category above (hollow balls). Solid boron clusters might also have comparable stability as being cut from the bulk, which is more stable than the sheet (α-bulk for instance is 0.4 eV/atom more stable than α-sheet). Recently it was reported that some stuffed boron fullerenes with larger sizes were more stable than B_{80}.[10] However, among the 80 atom clusters, B_{80} hollow fullerene was still the most stable.[10]

One reason for the unusually high cohesive energy of B_{80} (5.76 eV[1]) is, to our belief, its particular construction out of intercrossing B_{30} double-rings (DRs). DRs are special boron clusters since they appear as building blocks of boron nanotubes (BTs),[11] and also as the most stable among isomers with small size (from 20 to 36 atoms[12–17]). Other boron fullerenes made
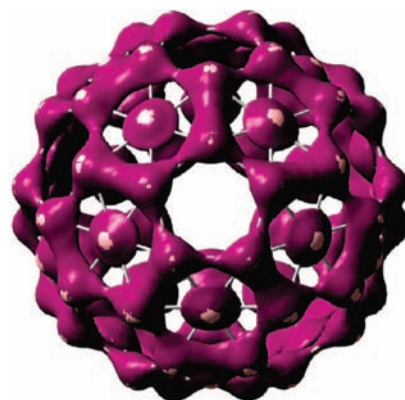

Figure 1. The B_{80} total electron density (Gaussian isovalue = 0.128).

out of DRs were explored recently by Szwacki.[18] While the quest for hollow boron balls is beginning, BTs have already been observed experimentally.[19] There is also evidence for the existence of B_{20} DR.[12,13]

Here we follow up with a detailed account the original report on B_{80},[1] which was mostly limited to its geometry and was intended for singling it out from a variety of hollow structures as the one with highest cohesive energy. First we discuss B_{80} precursors, i.e., sheet and DRs. In the first part of the results section we review different stable geometries of the sheet and compare the corresponding cohesive energies to that of B_{80}. Next we study DRs energetics and electronic structure in detail, since we feel these structures might be the key in stabilizing boron constructs. In the last part of section III we present a detailed analysis of the B_{80} symmetry, its possible isomers, electronic structure, and vibrational modes.

II. Methodology. The optimization of structures was performed within the density functional theory (DFT) framework, using generalized gradient approximation (GGA) for exchange and correlation functional PBE.[20] Results were obtained by allowing full relaxation of all atoms, using the plane-wave-based Quantum-ESPRESSO package[21] and ultrasoft Vanderbilt pseudopotentials.[22] The cutoff energy of 30 Ry for the plane-wave expansion and 210 Ry for the electronic charge density was

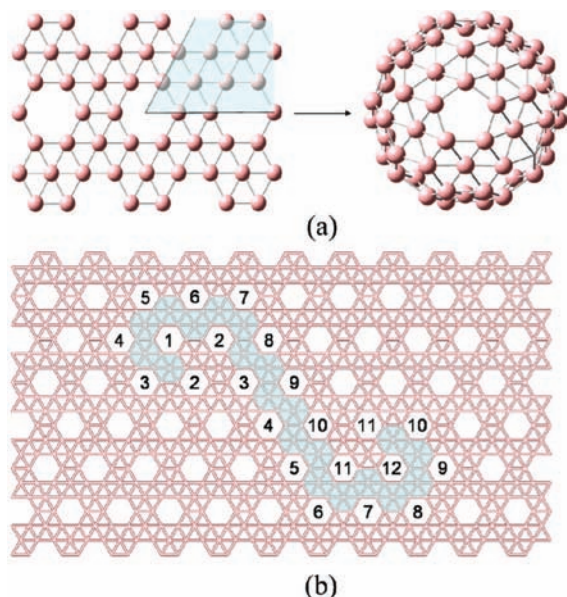* Corresponding author. E-mail: biy@rice.edu.

Figure 2. (a) Atoms in the shaded area of the α-sheet (left) are removed and the ones on the lines are identified to form pentagonal disclination in B_{80} (right). The figure shows only half of the molecule. (b) Projection of B_{80} on the α-sheet. Numbered facets represent the pentagons in B_{80}.

found to be sufficient to obtain converged results. The Γ point was used for the Brillouin zone integrations in the case of the finite structures, and $1 \times 1 \times 16$ ($1 \times 16 \times 16$) k-point sampling was used for the one (two)-dimensional infinite structures. The total energy was converged to 10^{-6} Ry and ionic positions were optimized until the forces acting on them were smaller than 10^{-3} Ry/Bohr. To study properties of finite structures, the supercell geometry was taken to be a cubic cell with lattice constant sufficiently large to avoid interactions between the clusters (allowing at least 12 Å distance between clusters). For electronic structure properties, molecular orbital (MO) and electron density (ED) images, and vibrational mode frequencies, the GAUSSIAN03 package[23] was used in conjunction with GaussView molecular visualization software. For DR electronic structure calculations we used the PBEPBE method and the all-electron 6-31G(d,p) basis set, to be consistent with the plane-wave results.[24] For careful analysis of energy and electronic structure of different isomers of B_{80}, optimizations were made by using a more accurate B3LYP/6-31G(d) method, and for frequency calculation, due to heavy computational demand, we used the same method but minimal basis set STO-3G.

III. Results and Discussion

We start by looking into structures related to B_{80}, i.e., boron sheet and double-rings.

1. Boron Sheet. Until recently, the most stable structure for the sheet was believed to be triangular. Flat triangular sheet turns out to be meta-stable. Triangular boron sheet becomes puckered.[25,26] Figure 3 shows the construction of this sheet. The values for cohesive energy (E_c), bond lengths (l_1 and l_2), and off-plane distance are summarized in Table 1. These values are based on our GGA results (using Quantum-ESPRESSO), which are in good agreement with previous reports.[25,26] In both cases (puckered and flat) the sheet is metallic, with no energy gap in the band structure.

Looking at the triangular lattice as a superpositioned honeycomb (graphene-like) lattice + centers, it was shown recently that removing 1/3 of the central atoms can further strengthen
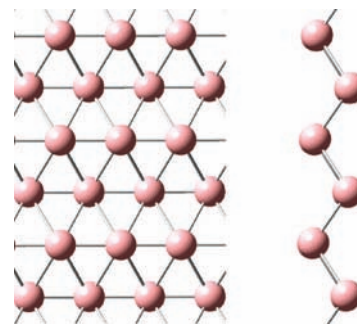

Figure 3. Top-view (left) and side-view (right) of the stable triangular boron sheet (puckered).

TABLE 1: Cohesive Energy (E_c), First Nearest Neighbor Bond Length (l_1, Horizontal in Figures 2 (α-Sheet) and 3 (Triangular Sheet)), Second Nearest Neighbor Bond Length (l_2, Diagonal), and the Off-Plane Distance (Projection of the l_2 Bonds on the Axis Normal to the Sheet)

	E_c (eV/atom)	l_1 (Å)	l_2 (Å)	off-plane distance (Å)
flat	5.62	1.70	1.70	0.0
puckered	5.84	1.62	1.88	0.93
α-sheet	5.93	1.70	1.70	0.0

the triangular units and help with stability.[6] The resulting structure, the α-sheet (Figure 2), is flat and metallic. Its values for bond length and cohesive energy obtained by the GGA method are given in Table 1.

The B_{80} cohesive energy (5.76 eV, using the same method[1]) is below the corresponding value for the α-sheet (5.93 eV), due to curvature strain energy.

2. Double-Rings. As we discussed briefly in the Introduction, we are interested in studying electronic and geometrical structure of DRs since (1) previous studies have shown that DRs are the most stable isomers of B_n for the cases studied with 36 atoms or less (i.e., $n = 20, 24, 32, 36$[13−17]), (2) they appear as building blocks of boron nanotubes,[11] and (3) the whole structure of B_{80} is made up of six crossing B_{30} DRs.

In this section we investigate DR clusters with various number of atoms ($n = 10$ to 40).

Geometry. The first nearest-neighbors (1NNs) of each B atom lie within the same ring, whereas the second nearest-neighbors (2NNs) are located on the opposite rings (except for $n = 10$, where we still use the same notation). Each atom has two 1NNs and two 2NNs. In Figure 4a we plot the 1NN and 2NN distances (l_{1NN} and l_{2NN}, respectively) versus the number n of atoms in the DR. From the figure one can see that l_{2NN} fluctuates for small n but stabilizes its value for $n \geq 32$, whereas l_{1NN} remains almost constant even for small n. The DR width (h) has a behavior similar to l_{2NN} since l_{1NN} is almost constant for different values of n. It is important to mention that most of the DRs with $n \leq 22$ are slightly distorted (for B_{10} and B_{14} the distortion is more pronounced). In Figure 4b we show the n-dependence of the average of two angles α and β, which each atom forms with its 1NNs and 2NNs, respectively (α lies on the plane perpendicular to the DR axis, whereas β lies on the DR surface). While α exhibits the expected values of regular polygonal angles, β exhibits fluctuations similar to that of l_{2NN} (which is expected since l_{1NN} remains constant). Note that B_{30} ($d = 7.7$ Å) has the smallest value for β (54.4°) and the largest value for l_{2NN} (1.754 Å) over all DRs.

Electronic Structure. The highest occupied molecular orbital (HOMO) and lowest unoccupied molecular orbital (LUMO) energy separation is an important measure of chemical stability. A molecule with small or no HOMO−LUMO gap is chemically
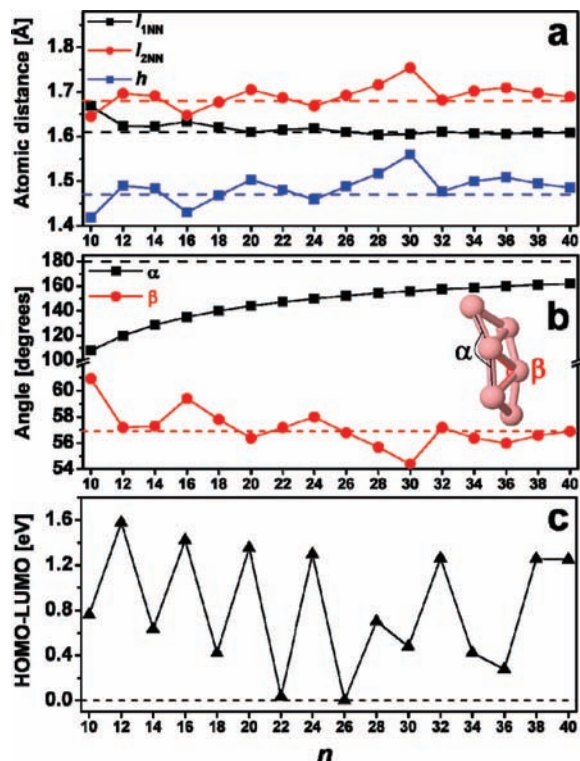
The Boron Buckyball and Its Precursors

J. Phys. Chem. A, Vol. 112, No. 51, 2008 **13681**

Figure 4. (a) First nearest neighbor distance (l_{1NN}, between atoms on the same ring), second nearest neighbor distance (l_{2NN}, between atoms on the opposite rings), and double-ring width (h) versus number of atoms (n). (b) The angles α (between the bonds made with the 1NNs) and β (between the bonds made with 2NNs) versus n. (c) HOMO−LUMO gap versus n.
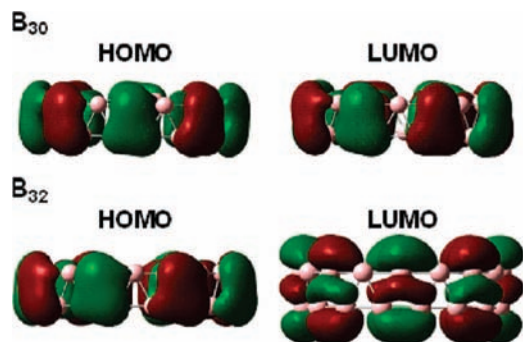

Figure 5. B_{30} (top) and B_{32} (bottom) HOMO and LUMO. Green (red) corresponds to positive (negative) values of the wave function.

reactive.[27,28] Theoretical basis for a close relationship between HOMO−LUMO gap and energy barriers to chemical reactions has been developed by Pearson and Parr and can be found in the literature.[28−30] In Figure 4c we plot the DR HOMO−LUMO gap versus the number of atoms. As we can see from the figure, the gap exhibits alternations similar to that known for metallic clusters.[31]

The HOMO and LUMO for $n = 30$ and 32 DRs are illustrated in Figure 5. In the case of $n = 32$, HOMO and LUMO are both doubly degenerate. They are both π-MOs with 3-center π bonds. HOMO corresponds mainly to s and p_y atomic orbitals (where y is the radial direction) and LUMO corresponds to s and p_z (where z is the axial direction). The two degenerate MOs are rotated by $\pi/8$ with respect to each other. In contrast, the HOMO and LUMO have the same shape and symmetry representation in the case of $n = 30$.

As we see from Figure 4c, there is no simple rule for large HOMO−LUMO gap; it can happen for $n = 4k$ or $4k + 2$ (k

being an integer). However, for relatively small diameters, a large gap occurs for $n = 4k$. Despite the pronounced fluctuations of the gap for small n, for bigger DRs the gap becomes small (0.342, 0.119, and 0.277 eV for B_{60}, B_{80}, and B_{110} DRs, respectively) and finally closes its value for infinite DR.

For the sake of completeness, we conclude this section with reporting the values of DR cohesive energy; it increases almost monotonously from 4.72 eV for B_{10} to 5.69 eV for infinite DR (or strip).[1] Comparing to the corresponding value for B_{80} (5.76 eV), we see that B_{80} is more stable than all the DRs. Also, it is worth noting that the B_{30} DR ($E_c = 5.57$ eV) is (considerably) further stabilized by intercrossing when fused to form B_{80} ($E_c = 5.76$ eV).

3. B_{80}. *Symmetry.* It was already mentioned in the Introduction that there are various isomers of boron buckyball, close to each other in energy and structure. Here we consider three B_{80} isomers obtained by B3LYP/6-31G(d) structural optimizations. Visually their geometries are almost identical;[2] however, a detailed analysis reveals important differences in their symmetries. Namely, two out of three structures under consideration are very close to having icosahedral (I_h) and tetrahedral (T_h) symmetries, while the third one appears to have no symmetry at all (C_1). Correspondingly, we denote these B_{80} isomers as I_h, T_h, and C_1. All the optimizations were performed without any symmetry restrictions, and our structures correspond to the true local minima of potential energy surface. The I_h isomer lies lowest, with a total energy of 3.6 meV lower than T_h and 30.3 meV lower than C_1 (the total energy differences are clearly very small and are sensitive to the method).

To estimate the deviations of I_h and T_h isomers from the corresponding ideal symmetries, let us consider the values of the dihedral angle between the six-membered ring and the plane formed by two of its atoms with the central boron atom. For the I_h isomer, the dihedral angles are from 3.26° to 3.81° (toward the center of the buckyball), i.e., their deviation from the average is negligible (less than 0.3°). In the case of the T_h structure, there is one group of 8 central atoms with dihedral angles of 8.88° to 9.07° toward the center, and another group of 12 central atoms with small ($\sim 1°$) dihedral angles away from the center. Our T_h isomer is similar to "isomer A" of ref 3 (one can see this reference for the description of its geometry). For comparison, the dihedral angles in the C_1 isomer vary from 7.54° toward the buckyball center to 1° away from it.

The symmetry is also reflected in electron charge transfer from central boron atoms to the B_{60} skeleton.[2] The amount of Mulliken charge transfer is 0.149 to 0.154 e in the I_h case, 0.063 to 0.065 e for the group of 8 atoms and 0.232 to 0.233 e for the group of 12 atoms in the T_h case, and in the range of 0.074 to 0.205 e in the C_1 case.

Finally, the symmetry of the B_{80} isomers under consideration is further confirmed by the analysis of their electronic structure.

Electronic Structure. There are a total of 200 occupied MOs in B_{80}. It is helpful to think of them as the linear combinations of the boron atomic orbitals (AOs), and to distinguish between the AOs belonging to the two nonequivalent groups of boron atoms, namely, the 20 atoms situated in the centers of hexagons and the 60 other atoms forming a structure analogous to C_{60}.

The lowest 80 MOs are linear combinations of 1s-AOs of boron atoms, with a negligible contribution of higher AOs. The 20 boron atoms in the centers of hexagons mainly contribute to the MOs 1−20, which have very close energies; the other 60 atoms mainly contribute to the MOs 21−80, which are also nearly degenerate.
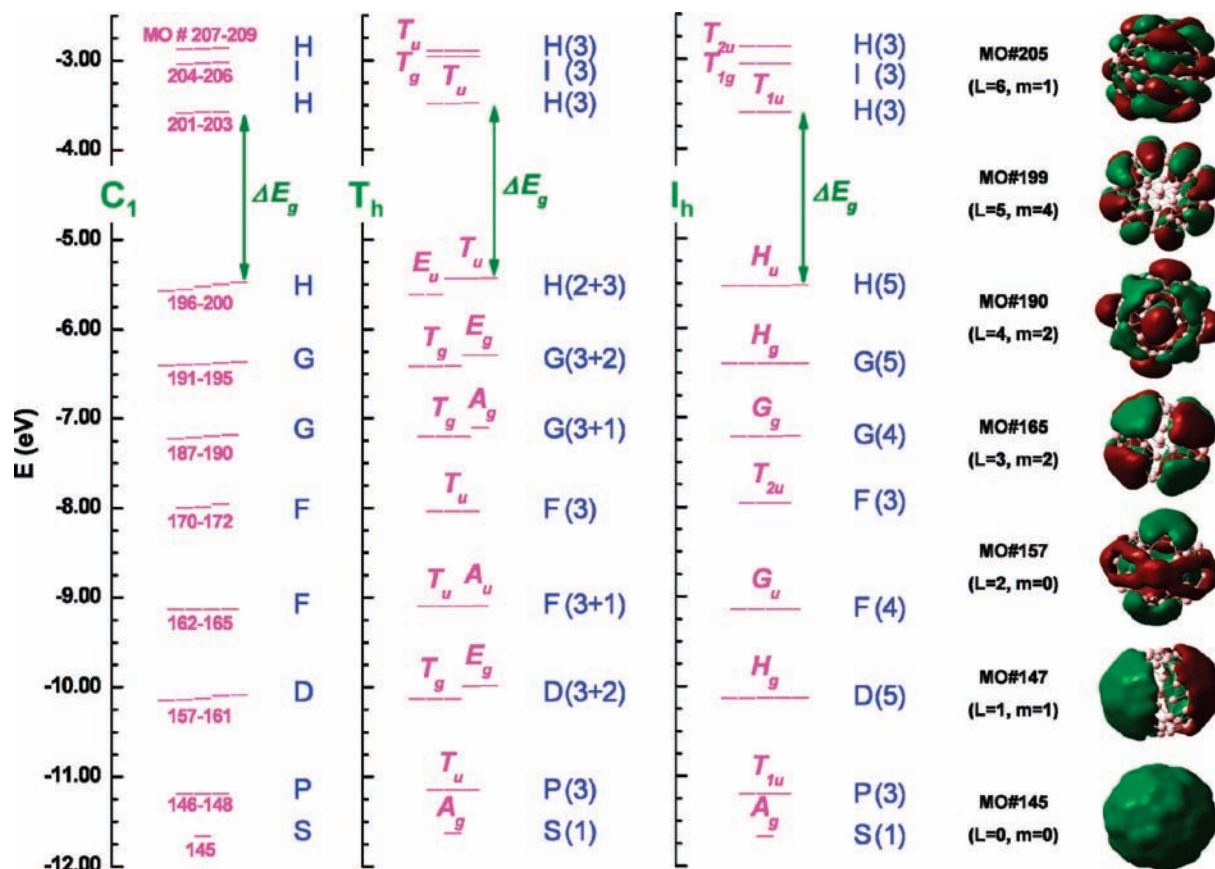
Figure 6. Energy diagram showing the π-type molecular orbitals of different isomers of B_{80}, calculated with the B3LYP/6-31G(d) method/basis. The left, middle, and right diagrams correspond to C_1, T_h, and I_h isomers, respectively. The levels with energy difference less than 10 meV are considered degenerate. The green arrow marks the HOMO–LUMO gap ($\Delta E_g = 1.88$, 1.95, and 1.93 eV for C_1, T_h, and I_h, respectively). For the energy levels of T_h and I_h structures, the corresponding representations are shown. For each type of spherical harmonics (S, P, D, etc.), the spatial distribution of one typical molecular orbital is shown in the right column (Gaussian isovalue = 0.01).

The higher occupied MOs of B_{80} are mostly made of boron 2s- and 2p-AOs and can have either σ or π character. There are only 60 π-electrons in the structure (which can be thought of as donated by the 60 equivalent boron atoms), and correspondingly, 30 π-orbitals are occupied.

Molecular orbitals of a nearly spherical molecule can be well approximated by the spherical harmonics,[32,33] and thus strongly resemble AOs of various types. The MOs having the azimuthal quantum number $L = 0$, 1, 2, 3, 4, 5, 6, etc. are commonly designated as S, P, D, F, G, H, I, etc. orbitals, analogous to the standard AO naming.

As the frontier molecular orbitals of B_{80} are of π-type, we concentrate on the π-MOs. Their energies for three isomers with C_1, T_h, and I_h symmetries are shown in Figure 6. One may compare this energy diagram with that of C_{60}.[32] Notice that the numbers of occupied π-orbitals in C_{60} and B_{80} both equal 30 and thus do not satisfy the $2(N + 1)^2$ Hirsch aromaticity rule,[34] because the H shell ($L = 5$) is not filled completely.

The rightmost column in Figure 6 shows the spatial distribution of one typical molecular orbital for each quantum number L.[35] The orbital degeneracy is determined by the azimuthal quantum number L and the symmetry of the molecule under consideration. For example, the 5-fold degenerate d-type atomic orbitals of transition metals split into a triplet and a doublet in the octahedral crystal field (see e.g., ref 36). Similarly, lowering the isomer symmetry from I_h to T_h leads to the orbital splitting, clear for instance for HOMO (MOs #196–200, H-type) in Figure 6. In particular, the symmetries of structures are reflected in their HOMO degeneracy: it is 5-fold for I_h (within 5 meV),

3-fold for T_h (within 2 meV), and nondegenerate for C_1. For the two symmetrical isomers, T_h and I_h, the representations of their symmetry groups are shown for all the π-type molecular orbitals in Figure 6.

Since the symmetric (I_h) structure has a nondegenerate ground state (HOMO is fully filled), the break of symmetry in other isomers is not due to the Jahn–Teller effect.

Vibrational Modes. To analyze the vibrational modes of boron buckyball, we resort to the B3LYP method with somewhat smaller STO-3G basis set[23] to keep the computational cost at bay. To make this analysis consistent, the B_{80} geometry should also be relaxed with the same method/basis. This yields a T_h symmetric isomer, close to "isomer B" of ref 3, with 12 (8) central atoms making dihedral angle ~12.5° (8°) toward (away from) the center. B_{80} has 64 distinct intramolecular mode frequencies in the range from 154 cm^{-1} for radial vibrations to 1181 cm^{-1} for tangential ones. The low-lying frequencies correspond to the central atom vibrations, suggesting the shallow nature of potential for their off-plane movement.

The breathing mode frequency is 474 cm^{-1}. In this mode, the 12 central hexagonal atoms with dihedral angle toward the center move in opposite phase with respect to the rest of the atoms. It is worth noting that in the Raman spectrum reported for BT samples,[19] there is a peak close to this value of frequency (~420 cm^{-1}). The authors of ref 19 also attribute the peaks at the range of 400 to 600 cm^{-1} to either smaller diameter BTs or to other boron structures present in the sample.

The Boron Buckyball and Its Precursors

J. Phys. Chem. A, Vol. 112, No. 51, 2008 **13683**

IV. Conclusions

In summary, we briefly reviewed the energetics and structure of a boron α-sheet in order to compare its cohesive energy to that of the B_{80} (which can be considered as the sheet wrapped on a sphere). We also investigated the geometry and electronic structure of double-rings to some detail, since they have a special place in boron chemistry. At last we examined the B_{80} from the MO energy level and symmetry point of view, as well as frequency modes. Analysis reveals that there are several minima around the icosahedral structure. The existence of different isomers close in energy to the original structure further lowers the free energy at some appropriate temperature. This will help in self-assembly of the atoms by increasing entropy and favoring the path to lowest free energy, which increases the likelihood of experimentally detecting B_{80} (since these different isomers' energies all lay within thermal fluctuations at room temperature).

Note Added in Proof. Rapid developments in the field call for adding a few important reports that came to our attention after completion of this work. A more comprehensive analysis of vibrational modes has recently been reported.[37] In ref 38, the authors also describe the I_h isomer's molecular orbital symmetries. A very recent work[39] classifies a family of boron fullerenes, which includes B_{80} and α-sheet as limits.

References and Notes

(1) Szwacki, N. G.; Sadrzadeh, A.; Yakobson, B. I. *Phys. Rev. Lett.* **2007**, *98*, 166804.

(2) Szwacki, N. G.; Sadrzadeh, A.; Yakobson, B. I. *Phys. Rev. Lett.* **2008**, *100*, 159901.

(3) Gopakumar, G.; Nguyen, M. T.; Ceulemans, A. *Chem. Phys. Lett.* **2008**, *450*, 175.

(4) Hawthorne, M. F. *Pure Appl. Chem.* **1991**, *63*, 327334.

(5) Dresselhaus, M. S.; Dresselhaus, G.; Eklund, P. C. *Science of Fullerenes and Carbon Nanotubes: Their Properties and Applications*; Academic Press: London, UK, 1996.

(6) Tang, H.; Ismail-Beigi, S. *Phys. Rev. Lett.* **2007**, *99*, 115501.

(7) Yang, X.; Ding, Y.; Ni, J. *Phys. Rev. B* **2008**, *77*, 041402.

(8) Singh, A. K.; Sadrzadeh, A.; Yakobson, B. I. *Nano Lett.* **2008**, *8*, 1314.

(9) Chernozatonskii, L. A.; Sorokin, P. B.; Yakobson, B. I. *JETP Lett.* **2008**, *87*, 489.

(10) Prasad, D. L. V. K.; Jemmis, E. D. *Phys. Rev. Lett.* **2008**, *100*, 165504.

(11) Quandt, A.; Boustani, I. *ChemPhysChem* **2005**, *6*, 2001.

(12) Oger, E.; Crawford, N. R. M.; Kelting, R.; Weis, P.; Kappes, M. M.; Ahlrichs, R. *Angew. Chem., Int. Ed.* **2007**, *46*, 8503.

(13) Kiran, B.; Bulusu, S.; Zhai, H.-J.; Yoo, S.; Zeng, X. C.; Wang, L.-S. *Proc. Natl. Acad. Sci. U.S.A.* **2005**, *102*, 961.

(14) Marques, M. A. L.; Botti, S. *J. Chem. Phys.* **2005**, *123*, 014310.

(15) Boustani, I.; Quandt, A. *Europhys. Lett.* **1997**, *39*, 527.

(16) Boustani, I.; Rubio, A.; Alonso, J. *Chem. Phys. Lett.* **1999**, *311*, 21.

(17) Chacko, S.; Kanhere, D. G.; Boustani, I. *Phys. Rev. B* **2003**, *68*, 035414.

(18) Szwacki, N. G. *Nano. Res. Lett.* **2008**, *3*, 49.

(19) Ciuparu, D.; Klie, R. F.; Zhu, Y.; Pfefferle, L. *J. Phys. Chem. B* **2004**, *108*, 3967.

(20) Perdew, J. P.; Burke, K.; Ernzerhof, M. *Phys. Rev. Lett.* **1996**, *77*, 3865.

(21) Baroni, S.; Corso, A. D.; Gironcoli, S. d.; Giannozzi, P.; Cavazzoni, C.; Ballabio, G.; Scandolo, S.:et al. http://www.pwscf.org/.

(22) Vanderbilt, D. *Phys. Rev. B* **1990**, *41*, 7892.

(23) Frisch, M J.; Trucks, G. W.; Schlegel, H. B.; Scuseria, G. E.; Robb, M. A.; Cheeseman, J. R.; Montgomery, J. A., Jr.; et al. *Gaussian 03*, revision B.03; Gaussian, Inc.: Wallingford, CT, 2004.

(24) Hariharan, P. C.; Pople, J. A. *Theor. Chim. Acta* **1973**, *28*, 213.

(25) Kunstmann, J.; Quandt, A. *Phys. Rev. B* **2006**, *74*, 035413.

(26) Lau, K. C.; Pandey, R. *J. Phys. Chem. C* **2007**, *111*, 2906.

(27) Hess, B. A.; Schaad, L. J. *J. Am. Chem. Soc.* **1971**, *93*, 2413.

(28) Pearson, R. G. *J. Am. Chem. Soc.* **1988**, *110*, 2092.

(29) Zhou, Z.; Parr, R. G. *J. Am. Chem. Soc.* **1990**, *112*, 5720.

(30) Pearson, R. G. *Proc. Natl. Acad. Sci. U.S.A.* **1986**, *83*, 8440.

(31) Jena, P.; Castleman, A. W., Jr. *Proc. Natl. Acad. Sci. U.S.A.* **2006**, *103*, 10560.

(32) Chen, Z.; King, R. B. *Chem. Rev.* **2005**, *105*, 3613.

(33) de Heer, W. A. *Rev. Mod. Phys.* **1993**, *65*, 611.

(34) Buhl, M.; Hirsch, A. *Chem. Rev.* **2001**, *101*, 1153.

(35) For comparison, see the extended table of atomic orbitals for the case $(n - l) = 2$, on the web-site http://www.orbitals.com/orb/orbtable.htm.

(36) Bersuker, I. B. *Electronic Structure and Properties of Transition Metal Compounds: Introduction to the Theory*; Wiley: New York, 1996.

(37) Baruah, T.; Pederson, M. R.; Zope, R. R. *Phys. Rev. B* **2008**, *78*, 045408.

(38) Ceulemans, A.; Muya, J. T.; Gopakumar, G.; Nguyen, M. T. *Chem. Phys. Lett.* **2008**, *461*, 226.

(39) Yan, Q. B.; Sheng, X. L.; Zheng, Q. R.; Zhang, L. Z.; Su, G. *Phys. Rev. B* **2008**, *78*, 201401 (R).